diminished anti-CD3-induced enteritis. Differences in the histopathology of enteritis induced by anti-CD3 in WT and CD30LKO mice were assessed at 24 h after injection. The absence of CD30L was associated with diminished anti-CD3-induced inflammation in the terminal ileum (Fig. 3B), with inhibition of reduction in the villous/crypt length ratio (Fig. 3C). Apoptotic bodies detected by TUNEL staining were counted in five villous crypt units of each group of WT and CD30LKO mice (Fig. 3D). The average number of apoptotic bodies in CD30LKO was significantly lower than that in WT mice (Fig. 3E). In addition, serum levels of IFN-γ (Fig. 4A), TNF-α (Fig. 4B), and IL-17 (Fig. 4C) in CD30LKO were significantly lower than those in WT mice. The level of IL-4 was not significantly altered (Fig. 4D). These results indicated that inflammation of the intestine induced by anti-CD3 antibody was reduced in the absence of CD30L/CD30 signals.

Recombinant Fusion Protein CD30–Ig Suppresses Anti-CD3-induced Enteritis

Recombinant fusion protein (CD30–Ig) contained the extracellular domain of CD30 fused to the hinge, CH2 and CH3 domains of murine IgG1, as described previously [6]. CD30–Ig has appropriate binding activity for the CD30L and blocks CD30L/CD30 signals. One hundred micrograms of CD30–Ig was administered to WT mice i.p. 1 h before and after injection of anti-CD3 mAb. The terminal ileum was removed from mice 24 h later, and tissue sections were stained with H&E and examined by optical microscopy (Fig. 5A). Enteritis was significantly reduced in mice that received CD30–Ig. Similar to the experiment with CD30LKO, villous crypt units were measured and villous/crypt length ratio was significantly greater in CD30–Ig-treated mice than in controls (Fig. 5B). Furthermore, the number of apoptotic bodies and the level of serum IFN-γ were also diminished in mice that received CD30–Ig (Fig. 5C and D).

Discussion

The role of CD30L/CD30 signals in mucosal immunity has not received much attention. Giacomelli et al. [16] have reported elevated levels of sCD30 in UC patients. On the contrary, in CD patients, the levels of sCD30 were not significantly higher than those of normal controls. They concluded that, as CD30-expressing cells produce Th2 cytokines, these differences come from the Th2 immune response in UC. Likewise, Elewaut et al. [20] have reported that lymphocytes obtained from UC patients overexpress CD30 when compared with those from CD patients. These studies have indicated that CD30L/CD30 signals play a more important role in UC than in CD. However, after the discovery of Th17 cells, Th reactions in human disorders need to be considered in a new axis of Th1/Th2/Th17 rather than a classical Th1/Th2 paradigm. Therefore, the involvement of Th2 reactions in the pathogenesis of UC needs to be re-evaluated. We thus considered that many issues remained to be investigated on the role of CD30L/CD30 signaling in IBD and conducted this current study. Contrary to a previous report, we found sCD30 levels were elevated in both CD and UC patients, and were correlated with disease activity. To clarify the reason for these contradictions, analysis of larger numbers of patients is needed. Nevertheless, our results suggest that CD30L/CD30 signals play some role in the development of intestinal inflammation in IBD.

Anti-CD3 antibody enteritis is induced purely by activated T cells. It is a useful murine enteritis model for discerning the role of T cells in enteritis. Merger et al. [19] have reported that apoptosis and mucosal injury are significantly reduced in perforin knockout mice, and a further significant reduction is observed in mice with perforin and Fas ligand (FasL) knockout. Both FasL and CD30L are members of the TNF superfamily. We have reported previously that the CD30 signal induces perforin expression [10]. Thus, we used the anti-CD3-induced enteritis model to analyze CD30L/CD30 signals in CD30LKO mice. As

expected, serum sCD30 increased at a peak of 24 h after anti-CD3 antibody injection. sCD30 recovered to normal levels at 72 h after injection of anti-CD3, with recovery of intestinal mucosa indicating that sCD30 level reflected severity of inflammation. These results suggest that reduced sCD30 after treatment in IBD patients is also caused by convergence of disease activity, and is not simply caused by immunosuppressants.

Recently, we have reported that oxazolone and TNBS induce colitis in CD30LKO mice [17]. We have found that CD30LKO mice are susceptible to oxazolone-induced colitis but are resistant to TNBS-induced acute colitis, and have concluded that CD30L plays a crucial role in deviating $CD30^+$ Th cells to Th1 cells in the colon [17]. In anti-CD3-induced enteritis, body weight loss, histological appearance and serum levels of IFN-γ and IL-17 were significantly suppressed in CD30LKO mice, which suggests that CD30L/CD30 signals deviate Th cells not only to Th1, but also to Th17 phenotype. In addition, CD30–Ig fusion protein, which blocks CD30L, significantly decreased disease activity of anti-CD3-induced enteritis in WT mice, which ruled out other genetic effects due to CD30L deletion in CD30LKO mice. Compared with the agonistic anti-CD30 mAb used in the former study [17], CD30–Ig fusion protein blocked CD30L/CD30 signals and was shown to be suitable for reduction of enteritis *in vivo*. These results suggest that blocking agent of CD30L/CD30 signaling, such as CD30–Ig or antagonistic anti-CD30 antibodies could be new therapeutic tools for IBD.

In summary, we showed that expression of sCD30 was elevated in patients with UC and CD, suggesting the involvement of CD30L/CD30 signaling in the pathogenesis of IBD. Using a murine enteritis model and recombinant protein CD30–Ig, we clarified that CD30L/CD30 signals play an important role in induction of enteritis in mice. We also introduced a new strategy for treatment of IBD and other diseases in which CD30L/CD30 signals are involved.

Acknowledgments

The authors wish to thank Dr. K. Croitoru and Dr. R. Borojevic for their helpful advice in the histological evaluation, and Dr. N. Aoi for his technical advice with ELISA.

References

1. Durkop H, Latza U, Hummel M, et al. Molecular cloning and expression of a new member of the nerve growth factor receptor family that is characteristic for Hodgkin's disease. *Cell.* 1992;68:421–427.

2. Smith CA, Gruss HJ, Davis T, et al. CD30 antigen, a marker for Hodgkin's lymphoma, is a receptor whose ligand defines an emerging family of cytokines with homology to TNF. *Cell.* 1993;73:1349–1360.

3. Hansen HP, Kisseleva T, Kobarg J, et al. A zinc metalloproteinase is responsible for the release of CD30 on human tumor cell lines. *Int J Cancer.* 1995;63:750–756.

4. Horie R, Watanabe T. CD30: expression and function in health and disease. *Semin Immunol.* 1998;10:457–470.

5. Gilfillan MC, Noel PJ, Podack ER, Reiner SL, Thompson CB. Expression of the costimulatory receptor CD30 is regulated by both CD28 and cytokines. *J Immunol.* 1998;160:2180–2187.

6. Bowen MA, Lee RK, Miragliotta G, Nam SY, Podack ER. Structure and expression of murine CD30 and its role in cytokine production. *J Immunol.* 1996;156:442–449.

7. Amakawa R, Hakem A, Kundig TM, et al. Impaired negative selection of T cells in Hodgkin's disease antigen CD30-deficient mice. *Cell.* 1996;84:551–562.

8. Cerutti A, Schaffer A, Shah S, et al. CD30 is a CD40-inducible molecule that negatively regulates CD40-mediated immunoglobulin class switching in non-antigen-selected human B

cells. *Immunity*. 1998;9:247–256.

9. Gruss HJ, Boiani N, Williams DE, et al. Pleiotropic effects of the CD30 ligand on CD30-expressing cells and lymphoma cell lines. *Blood*. 1994;83:2045–2056.

10. Muta H, Boise LH, Fang L, Podack ER. CD30 signals integrate expression of cytotoxic effector molecules, lymphocyte trafficking signals, and signals for proliferation and apoptosis. *J Immunol*. 2000;165:5105–5111.

11. Blazar BR, Levy RB, Mak TW, et al. CD30/CD30 ligand (CD153) interaction regulates CD4+ T cell-mediated graft-versus-host disease. *J Immunol*. 2004;173:2933–2941.

12. Nishimura H, Yajima T, Muta H, et al. A novel role of CD30/CD30 ligand signaling in the generation of long-lived memory CD8+ T cells. *J Immunol*. 2005;175:4627–4634.

13. Siminovitch KA. Advances in the molecular dissection of inflammatory bowel disease. *Semin Immunol*. 2006;18:244–253.

14. Kobayashi T, Okamoto S, Hisamatsu T, et al. IL23 differentially regulates the Th1/Th17 balance in ulcerative colitis and Crohn's disease. *Gut*. 2008;57:1682-1689.

15. Hölttä V, Klemetti P, Sipponen T, et al. IL-23/IL-17 immunity as a hallmark of Crohn's disease. *Inflamm Bowel Dis*. 2008;14:1175-1184.

16. Giacomelli R, Passacantando A, Parzanese I, et al. Serum levels of soluble CD30 are increased in ulcerative colitis (UC) but not in Crohn's disease (CD). *Clin Exp Immunol*. 1998;111:532–535.

17. Sun X, Somada S, Shibata K, et al. A critical role of CD30 ligand/CD30 in controlling inflammatory bowel diseases in mice. *Gastroenterology*. 2008;134:447–458.

18. Rachmilewitz D. Coated mesalazine (5-aminosalicylic acid) versus sulphasalazine in the treatment of active ulcerative colitis: a randomised trial. *BMJ (Clin Res Ed)*. 1989;298:82–86.

19. Merger M, Viney JL, Borojevic R, et al. Defining the roles of perforin, Fas/FasL, and tumour necrosis factor alpha in T cell induced mucosal damage in the mouse intestine. *Gut*.

2002;51:155–163.

20. Elewaut D, De Keyser F, Cuvelier C, et al. Distinctive activated cellular subsets in colon from patients with Crohn's disease and ulcerative colitis. *Scan J Gastroenterol.* 1998;33:743–748.

Figure legends

Fig. 1 Expression of sCD30 in serum of IBD patients. (A) Concentration of sCD30 in serum obtained from 12 healthy controls and 25 UC and 16 CD patients was analyzed by sCD30-specific ELISA. Open circles represent medians of each group. (B) Concentrations of serum sCD30 before and after treatment were compared in 9 UC and 5 CD patients. Open circles represent medians of each group. (C) Correlations of sCD30 and clinical scores in UC and CD are shown. $*P < 0.05$, CAI: clinical activity index, CDAI: Crohn's disease activity index.

Fig. 2 sCD30 expression in an anti-CD3-induced enteritis model. Time-course of sCD30 levels in mouse serum detected by ELISA at 0, 2, 4, 24 and 72 h after injection of anti-CD3. Serum sCD30 at 24 h after injection was significantly higher than that at 0 h.

Fig. 3 CD30LKO mice were resistant to anti-CD3-induced enteritis. (A) Body weight changes in WT and CD30LKO mice were measured every day after injection of anti-CD3 mAb. The body weight losses in CD30LKO mice were less than those in WT mice at days 2, 4, 5, 6 and 7 (average of five mice), $*P < 0.05$. (B) Histological findings of anti-CD3-induced enteritis in WT and CD30LKO mice. Terminal ileum was removed from mice injected with anti-CD3 mAb at 24 h after injection. Tissue sections were stained with H&E and examined by optical microscopy. (C) Five villous crypt units were measured in each mouse. The average villous/crypt length ratio was calculated from three mice in each group. (D) Terminal ileum was removed 24 h after injection, and apoptotic bodies were detected by TUNEL staining. (E) The number of apoptotic bodies was counted in five villous crypt units of each group of mice.

Fig. 4 Serum IFN-γ was measured in WT and CD30LKO mice at 4 h after anti-CD3 injection (A). Serum IFN-γ was higher in WT than CD30LKO mice. Serum TNF-α (B), IL-17 (C) and IL-4 (D) were measured in WT and CD30LKO mice at 2 h after anti-CD3 injection. N.S.: not significant

Fig. 5 Recombinant fusion protein CD30–Ig suppressed anti-CD3-induced enteritis. (A) CD30–Ig (100 μg) was injected i.p. 1 h before and after injection of anti-CD3 mAb. Terminal ileum was removed from mice at 24 h after injection of anti-CD3 mAb. Tissue sections were stained with H&E and examined by optical microscopy. (B) Five villous crypt units were measured in each mouse. The average villous/crypt length ratio was calculated from three mice in each group. (C) The number of apoptotic bodies was counted in five villous crypt units of each group of mice. (D) Serum IFN-γ was measured at 4 h after anti-CD3 antibody injection and was lower in mice with CD30–Ig injection.

Figure
Conflict of Interest.ClickHereToDownload

Figure 1

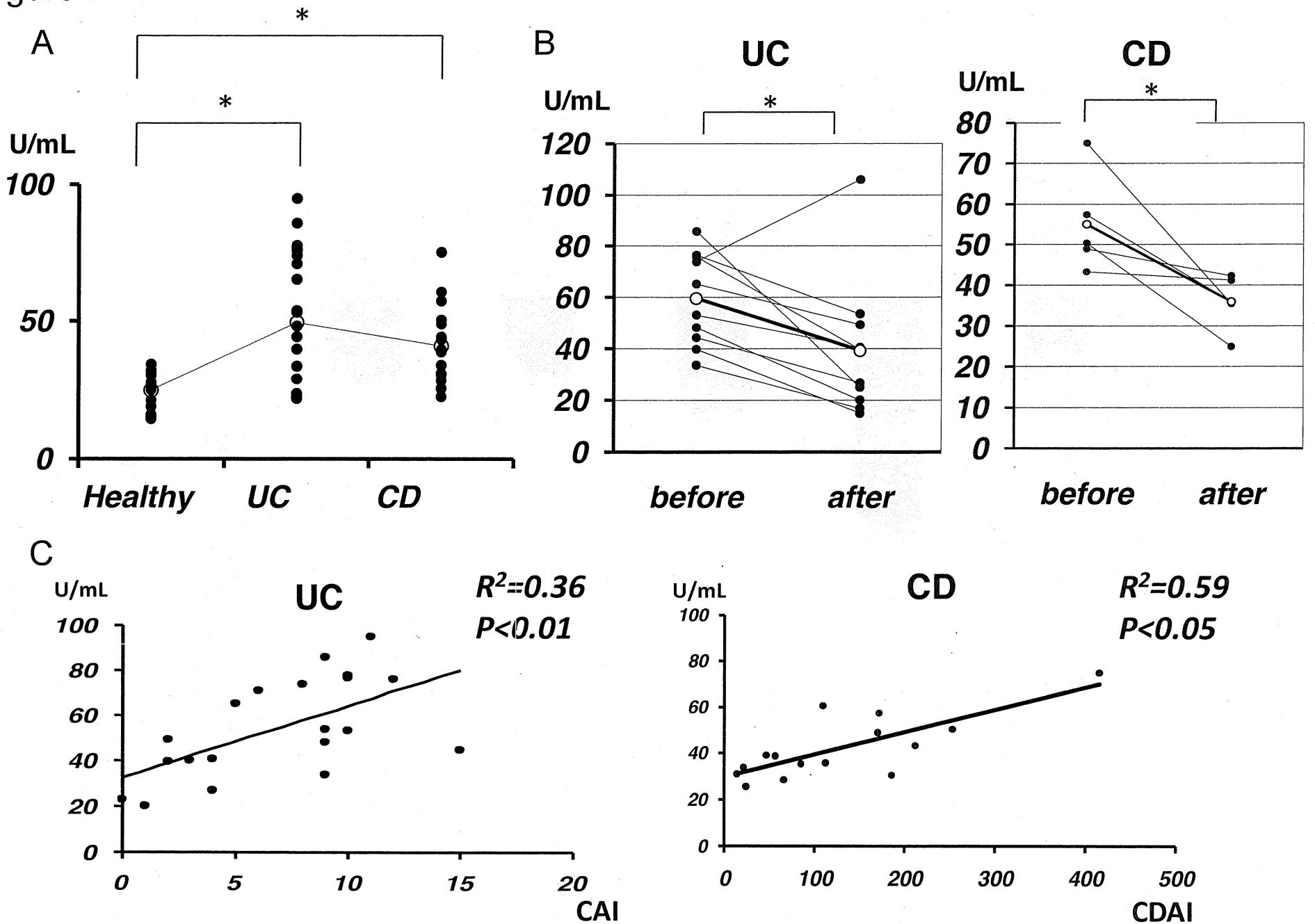

Figure 2

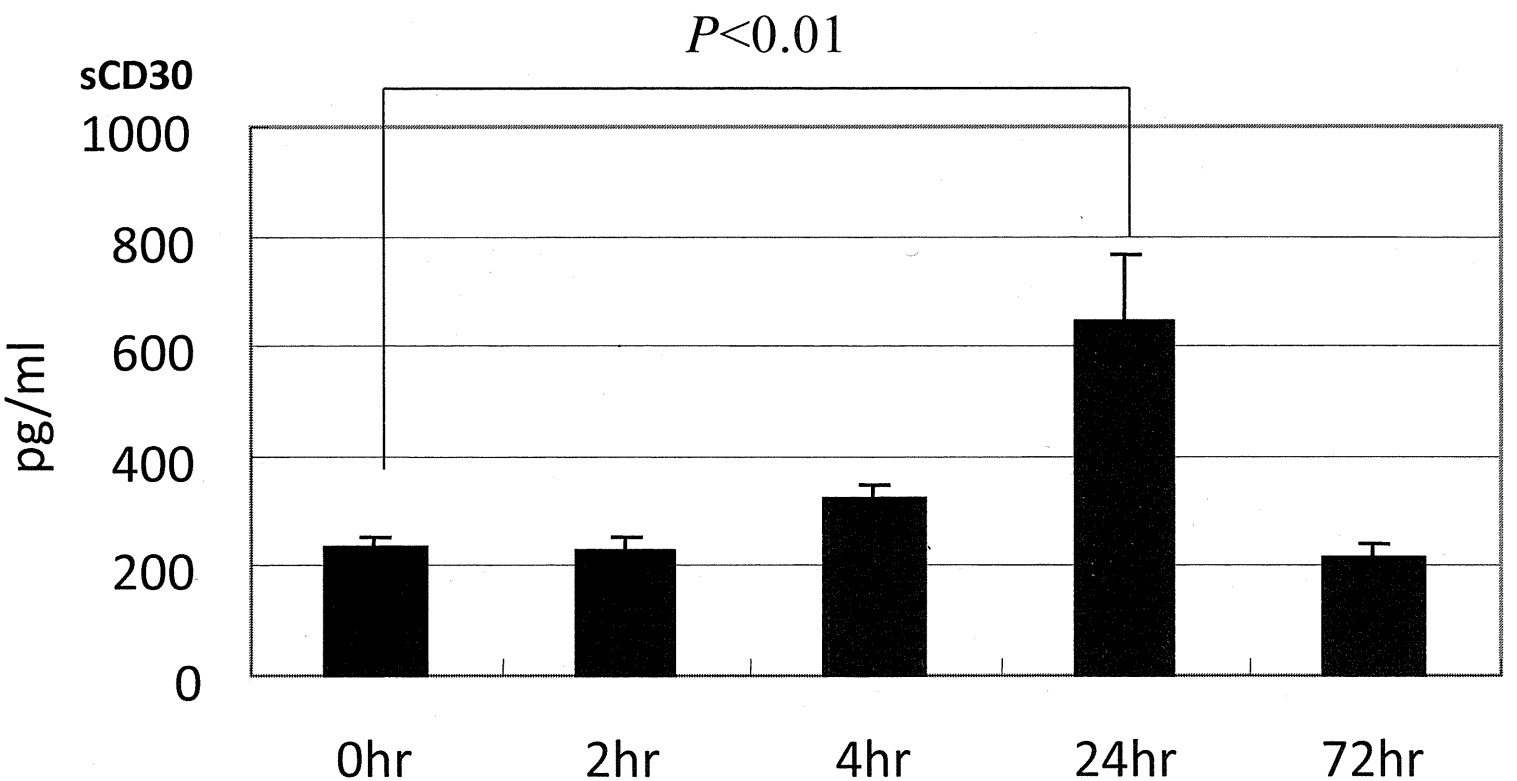

Figure 3

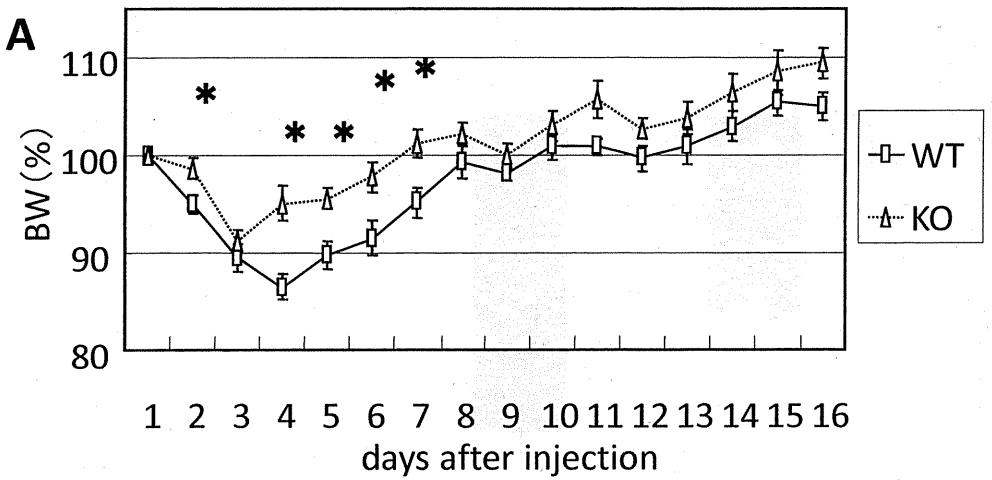
A
110
100
90
80
BW (%)
*
*
*
*
*
1 2 3 4 5 6 7 8 9 10 11 12 13 14 15 16
days after injection
WT
KO

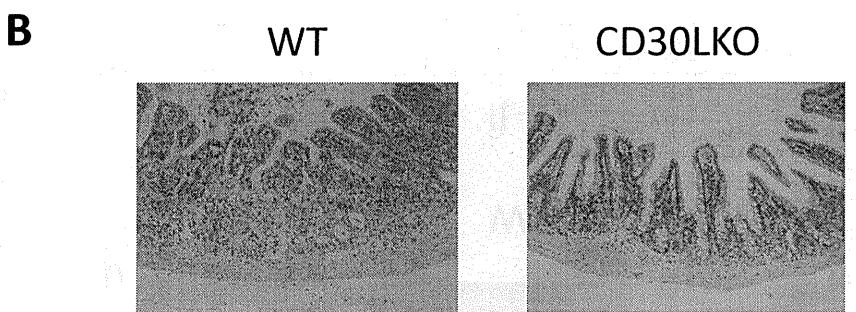
B
WT
CD30LKO

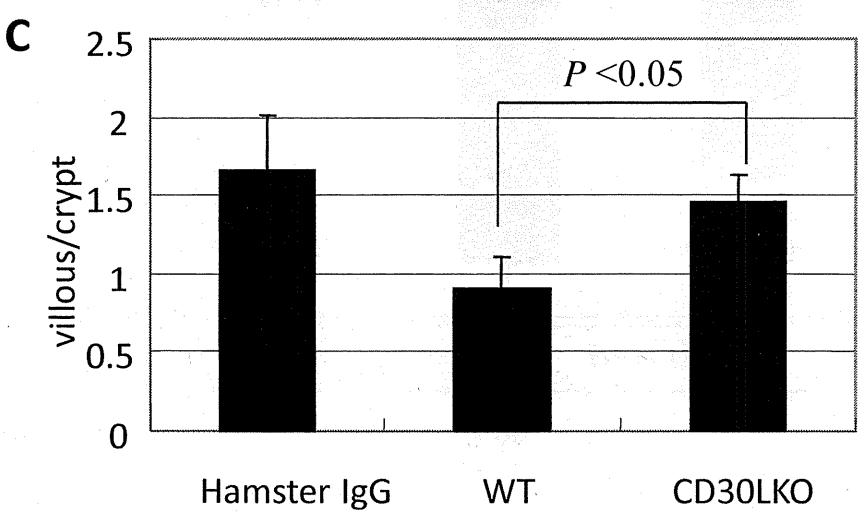
C
2.5
2
1.5
1
0.5
0
villous/crypt
P <0.05
Hamster IgG
WT
CD30LKO

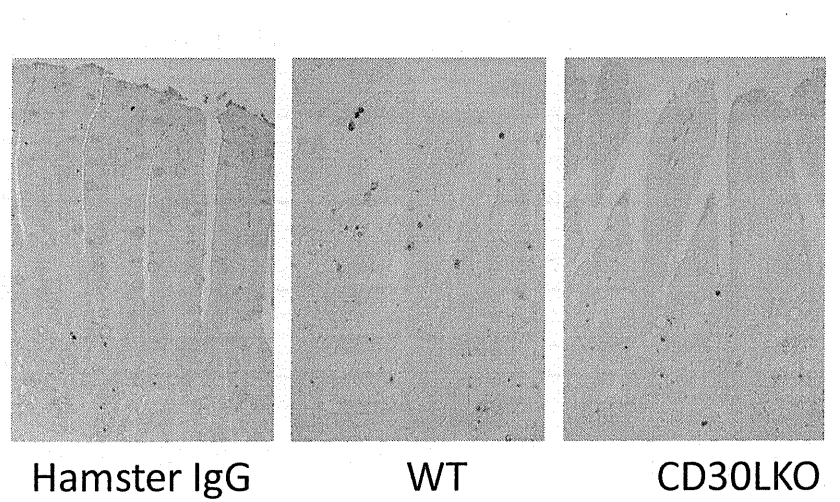
D
Hamster IgG
WT
CD30LKO

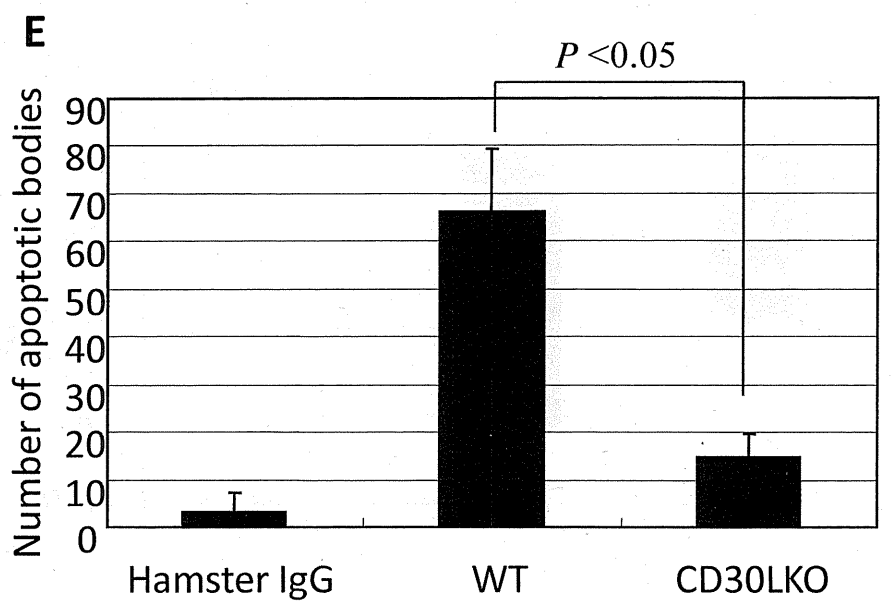
E
P <0.05
90
80
70
60
50
40
30
20
10
0
Number of apoptotic bodies
Hamster IgG
WT
CD30LKO

Figure 4

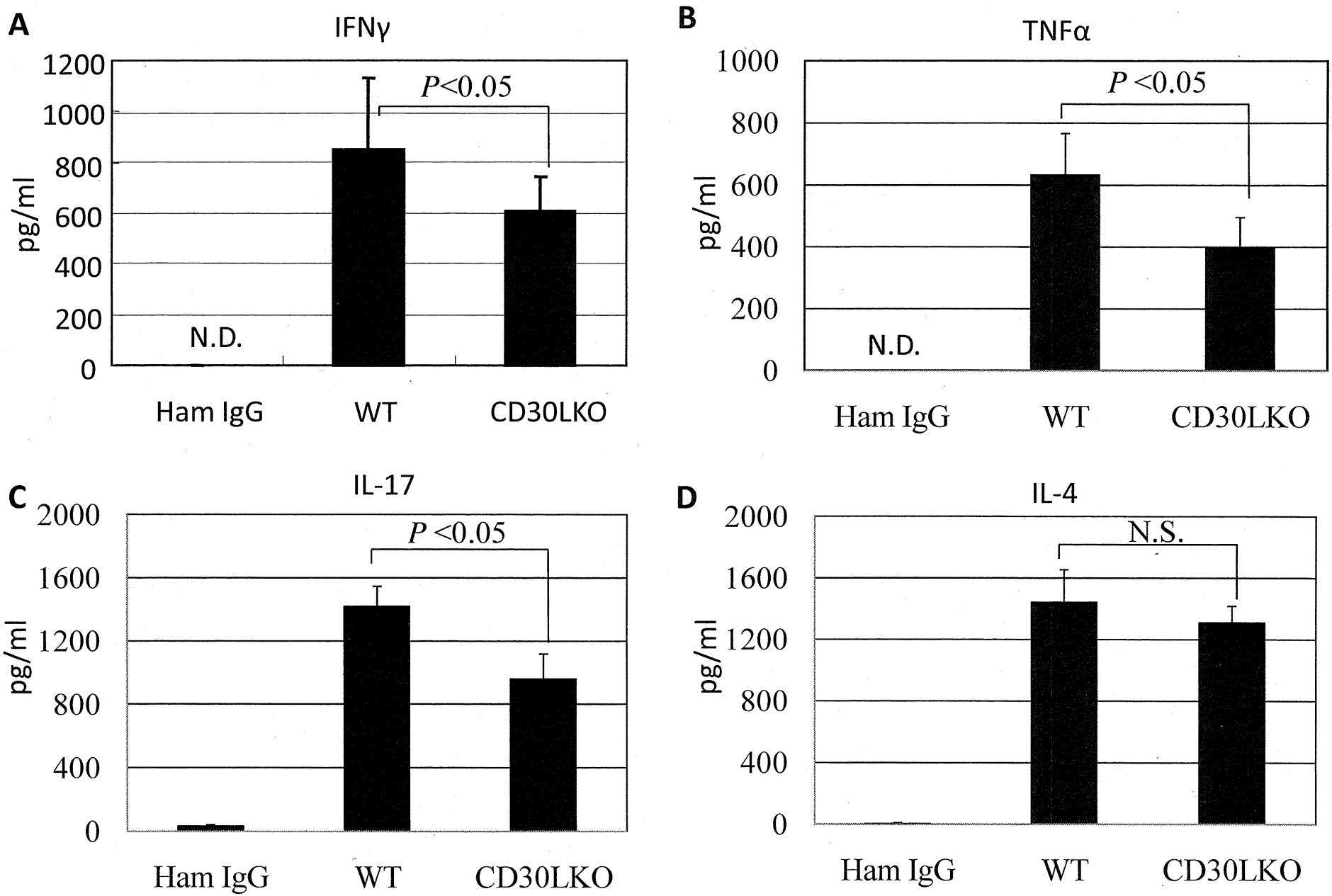
A
IFNγ
1200
1000
800
600
400
200
0
pg/ml
P<0.05
N.D.
Ham IgG
WT
CD30LKO
B
TNFα
1000
800
600
400
200
0
pg/ml
P <0.05
N.D.
Ham IgG
WT
CD30LKO
C
IL-17
2000
1600
1200
800
400
0
pg/ml
P <0.05
Ham IgG
WT
CD30LKO
D
IL-4
2000
1600
1200
800
400
0
pg/ml
N.S.
Ham IgG
WT
CD30LKO

Figure 5

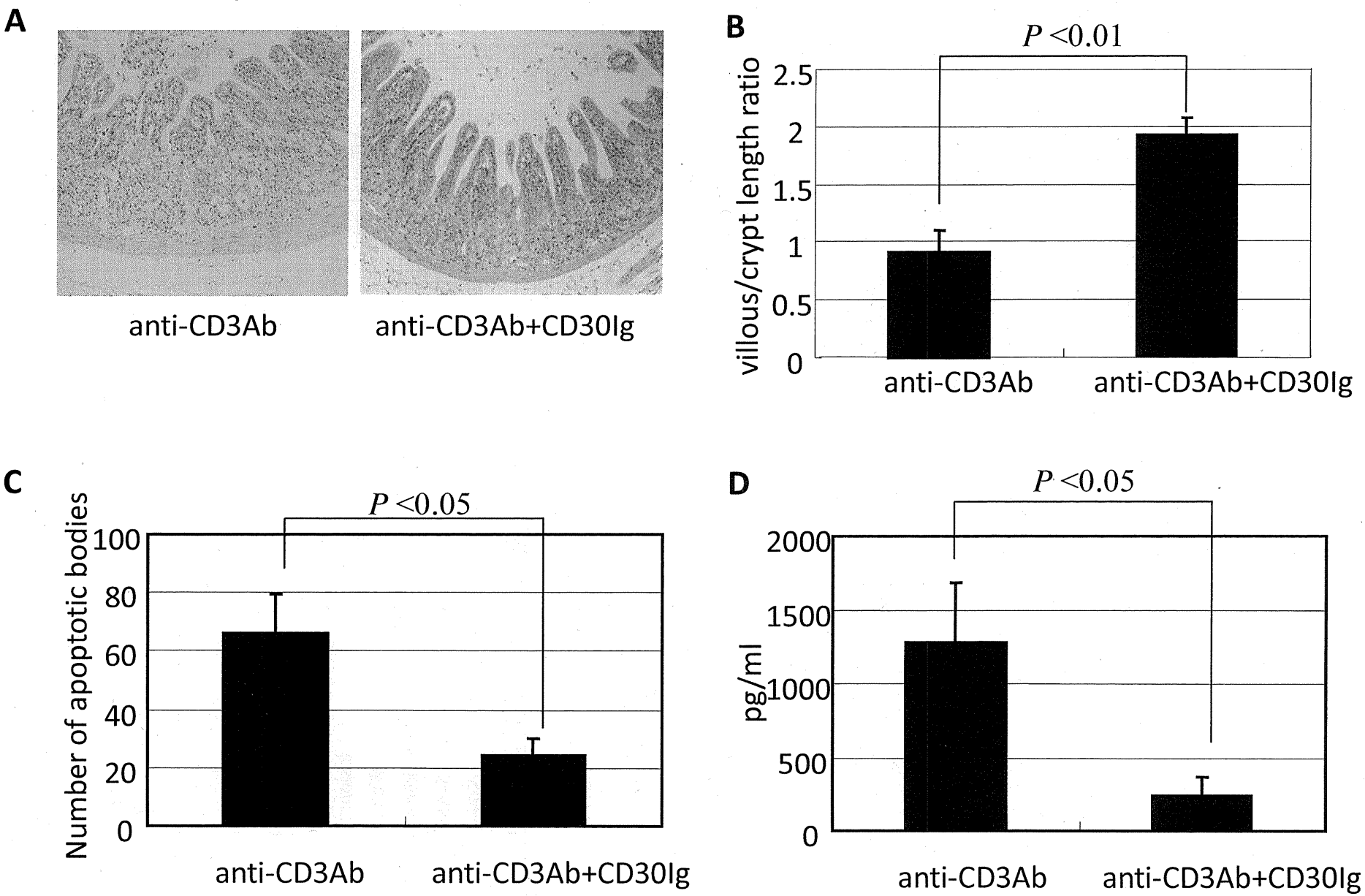
A
anti-CD3Ab
anti-CD3Ab+CD30Ig
B
P <0.01
villous/crypt length ratio
2.5
2
1.5
1
0.5
0
anti-CD3Ab
anti-CD3Ab+CD30Ig
C
P <0.05
Number of apoptotic bodies
100
80
60
40
20
0
anti-CD3Ab
anti-CD3Ab+CD30Ig
D
P <0.05
pg/ml
2000
1500
1000
500
0
anti-CD3Ab
anti-CD3Ab+CD30Ig

Table 1. Patient demographics

	Healthy controls	UC	CD
Number	12	25	16
Male:female	6:6	15:10	10:6
Age (yr; mean)	33.6	36.5	36.8
Affected area		Pancolitis: 19 Left-sided: 5 Proctitis:1	Without colonic lesion: 5 With colonic lesion: 11
treatment		5-ASA: 22 Steroid: 12 Apheresis: 7	5-ASA: 10 Steroid: 2 Infliximab: 1

ASA: 5-aminosalicylic acid

Open Journal of Blood Diseases, 2012, 2, 1-10
doi:10.4236/ojbd.2012.21001 Published Online March 2012 (http://www.SciRP.org/journal/ojbd)

Scientific Research

Leukemogenic Fusion Gene (p190 BCR-ABL) Transduction into Hematopoietic Stem/Progenitor Cells in the Common Marmoset

Yan Dong[1], Seiichiro Kobayashi[1], Yamin Tian[1,2], Manabu Ozawa[1,2], Takafumi Hiramoto[2], Kiyoko Izawa[1], Yuansong Bai[1], Yasushi Soda[1], Erika Sasaki[3], Toshio Itoh[3], Yoshiro Maru[4], Satoshi Takahashi[1], Kaoru Uchimaru[5], Naoki Oyaizu[6], Arinobu Tojo[1], Chieko Kai[7], Kenzaburo Tani[2*]

[1]Division of Molecular Therapy, Institute of Medical Science, The University of Tokyo, Tokyo, Japan; [2]Department of Molecular Genetics, Medical Institute of Bioregulation, Kyushu University, Fukuoka, Japan; [3]Central Institute for Experimental Animals, Kawasaki, Japan; [4]Department of Pharmacology, Tokyo Woman's Medical University, Tokyo, Japan; [5]Department of Hematology/Oncology, Research Hospital, Institute of Medical Science, The University of Tokyo, Tokyo, Japan; [6]Department of Laboratory Medicine, Research Hospital, Institute of Medical Science, The University of Tokyo, Tokyo, Japan; [7]Laboratory Animal Research Center, Institute of Medical Science, The University of Tokyo, Tokyo, Japan
Email: *taniken@bioreg.kyushu-u.ac.jp

Received December 9th, 2011; revised January 24th, 2012; accepted February 16th, 2012

ABSTRACT

Patients with Philadelphia chromosome (p190 BCR-ABL fusion gene)-positive acute lymphoblastic leukemia have a poor prognosis despite intensive therapeutic intervention. In this study, we attempted to develop a leukemia nonhuman primate model that mimics various human systems. Hematopoietic stem/progenitor cells in the common marmoset were transduced with a lentiviral vector containing the p190 BCR-ABL fusion gene by *ex vivo* transduction or *in vivo* direct bone marrow injection. In the latter model, BCR-ABL gene expression was maintained for more than one and a half years. One marmoset unexpectedly developed myelofibrosis-like disease. However, none of the marmosets have developed leukemia to date. In conclusion, we successfully achieved sustained p190 BCR-ABL gene expression *in vivo*. However, a genetic mutation in addition to p190 BCR-ABL may be required for the malignant transformation of hematopoietic stem/progenitor cells in the common marmoset during the short observation period. This novel *in vivo* approach will help develop a marmoset leukemia model in the future.

Keywords: Leukemia; Lentiviral Vector; Myelofibrosis; Common Marmoset

1. Introduction

Many preclinical *in vivo* studies have been conducted in mice because they are easy to breed and their biology and genetics are well-characterized. However, humans and mice differ genetically, pathophysiologically and pharmacokinetically, which makes it difficult to extrapolate the results from mouse models for direct clinical applications in humans. Large animals, especially nonhuman primates, are more closely related to humans. Moreover, because of their long life span, nonhuman primates can be treated and monitored over a long period, which presents opportunities for time-varying sampling of their blood and bone marrow. Thus, the development of non-human primate models that mimic human pathophysiology and pharmacokinetics will significantly further our understanding of human diseases. Particularly, genetically modified primates will be a powerful human disease model that can be used to preclinically assess the safety and efficacy of developing drugs.

Currently, Old World primates, such as the rhesus monkey (*Macaca mulatta*) and cynomolgus monkey (*Macaca fascicularis*), are commonly used for research [1-3]. However, these primates have several disadvantages, such as a slow sexual maturation period of approximately three years, fewer offspring over the female lifespan, and difficulty in handling.

The common marmoset (*Callithrix jacchus*) is a small New World primate that has attracted considerable attention as a potential animal for biomedical research [4,5]. The common marmoset is small, weighing approximately 350 - 400 g, relatively easy to breed, has a short gestation period of approximately 144 days, reaches sexual maturity at 12 - 18 months, and produces 40 - 80 offspring during the female lifespan. Thus, although marmosets are

*Corresponding author.

not as closely related to humans as apes or Old World primates, they are valuable as a potential primate model of human disease.

In this study, we attempted to establish a marmoset leukemia model by introducing a fusion gene that causes leukemia in humans. The Philadelphia chromosome (Ph) contains one of several forms of BCR and c-ABL gene fusions, and these fusions substantially contribute to the pathogenesis of chronic myelogenous leukemia (CML) and acute lymphoblastic leukemia (ALL). The p190 BCR-ABL fusion gene, in which BCR exon 1 is joined to ABL exon 2 (e1a2) and produces the p190 protein, is detected in 20% - 35% of ALL patients, and the prognosis of these patients is particularly poor [6,7]. Several treatments, such as allogeneic hematopoietic stem cell transplantation and novel small molecules that directly target the p190 BCR-ABL fusion gene have been developed to treat this refractory disease [8]. Transduction of the p190 BCR-ABL fusion gene is reportedly sufficient to cause leukemia in mice [9-11]. However, to date, there are no reports of a primate leukemia model. Establishing a marmoset model of this disease will be useful to test the efficacy of current and future treatments. Therefore, we transduced the p190 BCR-ABL fusion gene into marmoset $CD34^+$ hematopoietic stem/progenitor cells using a lentiviral vector and examined the occurrence of leukemogenic events.

2. Materials and Methods

2.1. Cell lines

Ba/F3 cells, a mouse interleukin-3 (mIL-3)-dependent hematopoietic cell line, were maintained in RPMI (Invitrogen, Carlsbad, CA, USA) supplemented with 10% fetal bovine serum (FBS) and mIL-3 (10 ng/mL) at 37°C in 5% CO_2 and passaged twice every week.

2.2. Animals and Preparation of Bone Marrow and Peripheral Blood Mononuclear Cells

Common marmosets were purchased from the Division of Animal Experimentation, Central Institute for Experimental Animals (Kawasaki, Japan), and bred at the animal center at our institute. In this study five animals were used including one control marmoset. No. 591 (male, 2 years and 6 months old) and No. 2338 (female, 4 years and 9 months old) were used as *ex vivo* BCR-ABL transduction models. No. 2129 (female, 5 years and 7 months old) and No. 2223 (female, 5 years and 3 months old) were used as BCR-ABL direct *in vivo* injection models. The study protocol was approved by the animal ethical committee of the University of Tokyo.

Bone marrow samples were collected by flushing the femurs of euthanized animals or aspirating the femoral bone marrow with an aspiration needle (Task, Tochigi, Japan). Peripheral blood samples were collected with heparin. Mononuclear cells (MNCs) in each sample were isolated by density-gradient centrifugation with Lymphoprep (Axis-Shield, Oslo, Norway). The cells were frozen in liquid nitrogen until further use.

2.3. Construction, Production and Transduction of Lentiviral Vector

Third generation, VSV.G pseudotyped lentiviral vectors were produced by transiently cotransfecting four plasmids into 293T cells as previously described [12]. Briefly, the p190 BCR-ABL fusion gene driven by a CMV or PGK promoter (HIV-CMV/PGK-BCR-ABL) was inserted into the transfer vector [13]. This plasmid was co-transfected into 293T cells using the calcium-phosphate method. The viral supernatant was harvested 48 and 72 hrs post transfection. The viral pellet was collected by ultra-centrifuging the supernatant and then stored at −80°C. The DNA titer, which is known to reflect the amount of transducible vector genome, was determined by real-time quantitative PCR as previously described [14]. For transduction, a cell pellet (2×10^5) was mixed and incubated with concentrated viral supernatant (20 μL) for 2 hrs in a 37°C incubator. The cells were generally infected *in vitro* with an MOI (multiplicity of infection) of 2.

2.4. Detection of p190 BCR-ABL Transgene Expression

RNA extraction and reverse transcription were performed as previously described using an RNA/DNA extraction kit (Qiagen, Hilden, Germany) and SuperScript First-Strand Synthesis System for RT-PCR (Invitrogen). Nested PCR amplification of p190 BCR-ABL was performed using a GeneAmp PCR System 9700 (Applied Biosystems, Foster City, CA, USA) with primers that specifically amplify the e1a2 transcripts. A 50 μL reaction mixture containing 2 mM of each dNTP, 25 mM $MgCl_2$, 10× PCR buffer, 0.5 μM primers, 1.25 U AmpliTaq Gold (Applied Biosystems) and 10 ng cDNA was subjected to 40 cycles of denaturation (95°C, 30 sec), annealing (61°C, 30 sec), and extension (72°C, 30 sec) and another 40 cycles with the inner primer set of denaturation (95°C, 30 sec), annealing (57°C, 30 sec), and extension (72°C, 30 sec). The final products were analyzed on a 1% agarose gel stained with ethidium bromide. The outer BCR-ABL primer set was forward primer (5'-CGC TCT CCC TCG CAG AAC TC-3') and reverse primer (5'-GGA GTG TTT CTC CAG ACT GTT GAC TG-3'), while the inner primer set was forward primer (5'-AAC AGT CCT TCG ACA GCA GCA-3') and reverse primer (5'-GCG TGA TGT AGT TGC TTG GGA-

3'). Sequencing analysis showed that the amplified products were compatible with the p190 BCR-ABL fusion gene (data not shown). Expression of p190 BCR-ABL protein was confirmed by western blot analysis in our previous report [15]. The glyceraldehyde-3-phosphate dehydrogenase (GAPDH) gene was simultaneously amplified as an internal control. In some experiments, real-time quantitative PCR analysis of p190 BCR-ABL was performed as previously described [16].

2.5. Enrichment of $CD34^+$ Bone Marrow Cells

Marmoset bone marrow $CD34^+$ cells were isolated with the immunobeads system using streptavidin microbeads (MACS, Miltenyi Biotec, Sunnyvale, CA, USA). Marmoset bone marrow MNCs were prepared from fresh bone marrow samples and stained with a biotin-labeled anti-marmoset CD34 monoclonal antibody (clone MA24) for 30 min at 4°C [17]. The cells were washed and incubated with streptavidin-conjugated microbeads for 15 min at 4°C. The $CD34^+$ cells were washed and separated using immunomagnetic columns (MACS) according to the manufacturer's instructions.

2.6. *Ex Vivo* p190 BCR-ABL Transduction and Autologous Peripheral Blood Stem Cell Transplantation (PBSCT)

The time course and treatment protocol are described in **Table 1**. Briefly, 10 μg/kg/day of recombinant human granulocyte colony-stimulating factor (G-CSF, Roche, Basel, Switzerland) was subcutaneously administered to individual marmosets for five days. Peripheral blood (1 mL) was collected daily from the femoral vein of each marmoset for seven consecutive days. MNCs were isolated by Ficoll-Hypaque centrifugation. Red cell lysis was performed when necessary. The cells were frozen using a programmed freezer and stored in liquid nitrogen until use. Ninety milligrams of busulfan (Sigma Aldrich, St Louis, MO, USA) was dissolved in 15 mL of DMA/PEG (1:2) solution, and a 6 mg/mL busulfan solution was made. All marmosets received the busulfan solution (10 mg/kg) from day −3 to day −2 before PBSCT as previously described [18,19].

Three days before transplantation, the MNCs were thawed and incubated overnight in IMDM supplemented with 10% FBS and human cytokines (10 ng/mL hSCF, hIL-3 and hTPO) as previously described with some modifications [12]. After pre-stimulation, the cells were collected and centrifuged. The cell pellet was incubated with the concentrated viral supernatant at 37°C in 5% CO_2 for 2 hrs. The cells of two marmoset (No. 591 and 2338) were infected with the CMV-p190 BCR-ABL lentiviral vector. Then, the cells were cultured in IMDM supplemented with 10% FBS and human cytokines (hSCF, hIL-3, hTPO) in 24-well plates for 48 hrs. The transduced cells were collected, filtered with 40 μm nylon mesh, washed with serum-free IMDM and suspended in 1.5 mL normal saline. The cells (2×10^6) were transplanted via the femoral vein using a syringe and 27 G needle.

2.7. Direct Injection of Lentiviral Vectors into the Bone Marrow

The time course and treatment protocol are described in **Table 2**. Briefly, marmosets received 25 mg/body of 5-fluorouracil (Kyowa Hakko Kirin, Tokyo, Japan) on day −5 and prednisolone from day −3 to day 1. After anesthesia, *in vivo* transduction of bone marrow cells was performed by directly injecting the viral supernatant into the bone marrow cavity using an aspiration needle on day 0. One marmoset (No. 2129) received the CMV-p190 BCR-ABL lentiviral vector, whereas the other (No. 2223) received the PGK-p190 BCR-ABL lentiviral vector. All marmosets received both oral fluconazol (2 mg/body/day) and intramuscular injections of ampicillin (10 mg/body/day) from day −5 to day 7 and pentamidine (1.5 mg/body/day) once on day −5.

2.8. Colony Formation Assay

A colony formation assay (progenitor cell assay) was performed as previously described with minor modifications [17]. Bone marrow cells were washed twice, plated in methylcellulose containing human hematopoietic

Table 1. Time coure and treatment of *ex vivo* BCR-ABL transduction method.

Treatment	−14	−13	−12	−11	−10	−9	−8	−7	−6	−5	−4	−3	−2	−1	0	(days)
G-CSF (10 μg/body)	•	•	•	•	•											
PBMC collection					•	•	•	•	•	•	•					
Busulfan (10 mg/body)												•	•			
ex vivo gene transduction (p190 BCR-ABL)													•	•		
PBSCT															▼	

G-CSF: granulocyte colony stimulationg factor; PBMC: peripheral blood mononuclear cell; PBSCT: peripheral blood stem cell transplantation.

Table 2. Time coure and treatment of BCR-ABL direct *in vivo* injection method.

Treatment	–5	–4	–3	–2	–1	0	1	2	3	4	5	6	7	(days)
5FU (25 mg/body)	•													
PSL (8 mg/body)			•	•	•									
PSL (4 mg/body)						•								
PSL (2 mg/body)							•							
BM injection (p190 BCR-ABL)						▼								
Pentamidine (1.5 mg/body)	•													
ABPC (10 mg/body)	•	•	•	•	•	•	•	•	•	•	•	•	•	
FCZ (2 mg/body)	•	•	•	•	•	•	•	•	•	•	•	•	•	

5FU: 5-fluorouracil, PSL: predonisolone, BM: bone marrow, ABPC: ampicillin, FCZ: fluconazole

cytokines (Methocult GF+, StemCell Technologies, Vancouver, BC, Canada) and incubated at 37°C in 5% CO_2. Then, 1.5×10^3 MACS-sorted $CD34^+$ cells or 3×10^4 non-sorted cells were plated in one dish. On day 14, individual colonies were picked to identify BCR-ABL gene transduction by RT-PCR and examined by May-Giemsa staining.

3. Results

3.1. Lentiviral Vector Expressing p190 BCR-ABL Functionally and Efficiently Transduced Hematopoietic Stem/Progenitor Cells

First, we produced third generation VSV.G pseudotyped lentiviral vectors expressing the p190 BCR-ABL fusion gene (HIV-CMV/PGK-BCR-ABL). Plasmids including the lentiviral transfer vector were transduced into 293T cells by the calcium phosphate method. After 48 and 72 hrs, the viral supernatants were collected and ultra-centrifuged. The DNA titers of HIV-CMV-BCR-ABL and HIV-PGK-BCR-ABL were 5.59×10^7/ml and 2.53×10^8/ml, respectively. To determine that the vector functions properly, Ba/F3 cells, a mIL-3-dependent murine hematopoietic cell line, were transduced with this vector and cultured without mIL-3. These cells rapidly expanded after 12 days, indicating that p190 BCR-ABL gene expression allowed the Ba/F3 cells to grow autonomously regardless of the promoter used (**Figure 1(a)**). RT-PCR confirmed that p190 BCR-ABL was expressed in the transduced Ba/F3 cells (**Figure 1(b)**). We then performed quantitative RT-PCR (**Figure 1(c)**). Although the MOI of the lentiviral vector was not high, p190 BCR-ABL expression was detected in the Ba/F3 cell line. Next, to check whether marmoset hematopoietic stem/progenitor cells were efficiently transduced with the lentiviral vector, MACS-sorted bone marrow $CD34^+$ cells were transduced with the lentiviral vector (HIV-CMV/PGK-BCR-ABL) and subjected to the colony formation assay (**Figure 1(d)**). In more than 80% of colonies examined, p190 BCR-ABL transduction was detected regardless of the promoter. Taken together, the above findings indicate that this oncogene was efficiently transduced into marmoset stem/progenitor cells.

3.2. *Ex Vivo* BCR-ABL Transduction Method

To establish a marmoset leukemia model, we first tried the *ex vivo* BCR-ABL transduction method (**Table 1**). After mobilizing the hematopoietic stem/progenitor cells by administering G-CSF, peripheral blood MNCs were collected according to the schedule in **Table 1**. The collected cells were pre-cultured with cytokines (10 ng/ml hSCF, hIL-3 and hTPO) to improve the transduction efficiency. After the cells were transduced with the lentiviral vector containing the p190 BCR-ABL fusion gene *ex vivo*, they were transplanted into common marmosets that were previously treated with pre-conditioning busulfan (**Table 1**). On days 28 and 56 post transplantation, BCR-ABL expression was detected by RT-PCR in the peripheral blood MNCs of two marmosets (**Figure 2(a)**, upper). The time course for BCR-ABL expression after transplantation is shown in **Figure 2(a)** (lower). Although we expected stable BCR-ABL expression, BCR-ABL expression disappeared after days 56 and 100 in two marmosets. Because this result was thought to partially result from low-level transgene expression due to ineffective gene transduction in hematopoietic stem/progenitor cells, we changed the gene transduction method.

3.3. *In Vivo* BCR-ABL Direct Transduction Method

Previous reports showed that directly injecting lentiviral vectors *in vivo* resulted in stable gene expression [20].

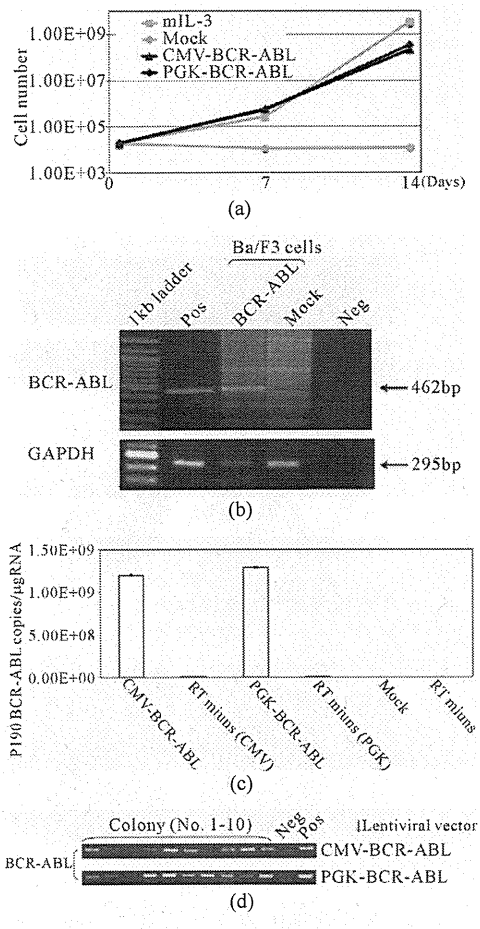

Figure 1. (a) Ba/F3, a murine hematopoietic cell line that is dependent on mouse interleukin-3 (mIL-3), was transduced with the p190 BCR-ABL lentiviral vector (HIV-CMV/ PGK-BCR-ABL) and cultured without mIL-3. As positive and negative controls, mock transfected cells were cultured with or without mIL-3. The number of live cells was determined by the trypan blue exclusion method. All experiments were done in triplicate and also repeated three independent times, and data were plotted as mean ± SD; (b) Detection of the BCR-ABL fusion gene in transduced Ba/F3 cells. Three days after lentiviral transduction, RT-PCR for the BCR-ABL gene was performed in BCR-ABL- or mock-transduced cell lines. Pos: positive control (KOPN30 cell line harbouring p190 BCR-ABL), Neg: negative control (ddw: deionized distilled water); (c) Quantitative analysis of transduced p190 BCR-ABL fusion gene expression. Three days after lentiviral transduction, quantitative RT-PCR for p190 BCR-ABL was performed. RT minus indicates the control PCR reaction without reverse transcriptase; (d) Lentiviral transduction of the BCR-ABL gene into colony-forming hematopoietic stem/progenitor cells. MACS-sorted marmoset CD34$^+$ cells were transduced with the lentiviral vector expressing p190 BCR-ABL under a CMV or PGK promoter, and then 1.5 × 10^3 cells were plated in methylcellulose containing human hematopoietic growth factors. After 14 days of culture, colonies were randomly picked and examined for BCR-ABL gene expression by RT-PCR.

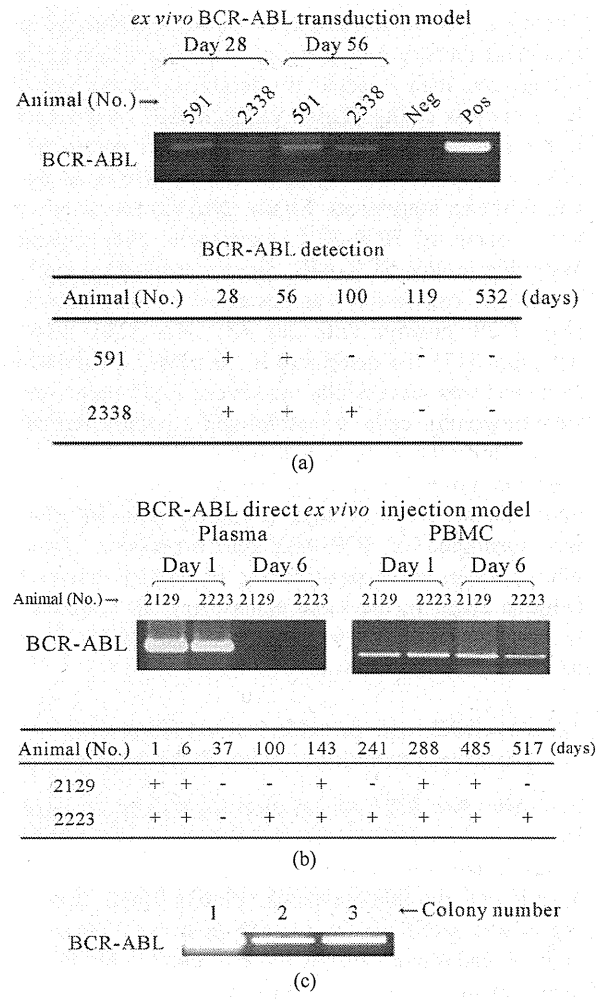

Figure 2. (a) Detection of the BCR-ABL fusion gene with the *ex vivo* BCR-ABL transduction method. Upper: RT-PCR of the BCR-ABL fusion gene in samples on day 28 and 56 after the BCR-ABL-transduced CD34$^+$ cells were transplanted. Lower: detection of BCR-ABL in samples from day 28 to 532 in two marmosets. BCR-ABL expression disappeared in two marmosets after day 56 and 100. GAPDH expression was confirmed for all samples (data not shown). No. 591 and No. 2338: CMV-p190 BCR-ABL; (b) Detection of BCR-ABL fusion gene with the *in vivo* BCR-ABL direct transduction method. Upper: RT-PCR of the BCR-ABL fusion gene in plasma and PBMC samples on days 1 and 6. Lower: detection of BCR-ABL in samples from day 1 to day 517 in two marmosets. Compared to the *ex vivo* BCR-ABL transduction method, two marmosets maintained long-term BCR-ABL expression. No. 2129: CMV-p190 BCR-ABL. No. 2223: PGK-p190 BCR-ABL; (c) Detection of the BCR-ABL fusion gene in colony-forming hematopoietic stem/progenitor cells. Bone marrow MNCs were isolated from marmoset No. 2223 on day 517, and 3 × 10^4 cells were plated in methylcellulose containing several human hematopoietic growth factors. After 14 days of culture, colonies were randomly picked and examined for the BCR-ABL gene. Three out of nine colonies were positive for BCR-ABL.

Therefore, we administered an immunosuppressive pretreatment therapy consisting of 5-fluouracil and prednisolone and then injected the lentiviral vector into the bone marrow cavity (**Table 2**). BCR-ABL was detected in the plasma on day 1 but not day 6. In contrast, BCR-ABL was detected in peripheral blood MNCs on day 1 and 6 in two marmosets. **Figure 2(b)** (lower) shows the time course of BCR-ABL expression after injection. With this *in vivo* BCR-ABL direct transduction method, BCR-ABL expression was sustained in two marmosets (No. 2129: positive until day 485, No. 2223: positive until day 517). To determine if the p190 BCR-ABL fusion gene was successfully transduced into hematopoietic stem/progenitor cells, we performed a colony formation assay. Thirty thousand bone marrow MNCs were isolated from marmoset No. 2223 on day 517 and plated in methylcellulose. After 14 days of culture, random colonies were examined for BCR-ABL gene expression. Three of nine colonies were positive for BCR-ABL expression (**Figure 2(c)**). In the same experiment, all colonies for the control marmoset were negative for BCR-ABL expression (data not shown).

3.4. Myelofibrosis in a Marmoset That Was Directly Transduced with BCR-ABL *in Vivo*

Marmoset No. 2223, which received a direct *in vivo* injection and maintained BCR-ABL expression, became lethargic and lost weight. A blood cell count indicated anemia and thrombocytopenia (**Figure 3(a)**). This marmoset was sacrificed on day 686 post injection and examined pathologically. BCR-ABL expression was detected in the spleen, liver, kidney, heart and peripheral blood MNCs by RT-PCR. However, the bone marrow sample was negative for BCR-ABL. Hematoxylin-Eosin staining of the bone marrow showed that the bone marrow cavity was replaced by a marked noncellular component (**Figure 3(b)**). Bone marrow fibrosis was confirmed by Masson staining. An examination of the liver revealed extramedullary hematopoiesis. Naphthol AS-D chloroacetate (ASD) and Myeloperoxidase (MPO) staining confirmed that the cells were of myeloid lineage (**Figure 3(c)**).

4. Discussion

Previously, we reperted the usefulness of the common marmoset as a hematopoietic stem/progenitor cell transplantation model, analytic results of major histocompatibility antigens, and the production of anti-marmoset CD34 monoclonal antibodies[4,17,21,22]. These studies helped to establish and analyze a primate disease model. In this study, we lentivirally transduced common marmoset hematopoietic cells with the p190 BCR-ABL fu-

Animal (No.)	RBC ($\times 10^4/\mu L$)	WBC ($\times 10^2/\mu L$)	Plt ($\times 10^4/\mu L$)
BCR-ABL (2223)	175	13.9	14.1
Normal	623±74	9.7±3.2	65.0±17.0
(range)	(373-717)	(3.3-17.4)	(40.5-111.2)

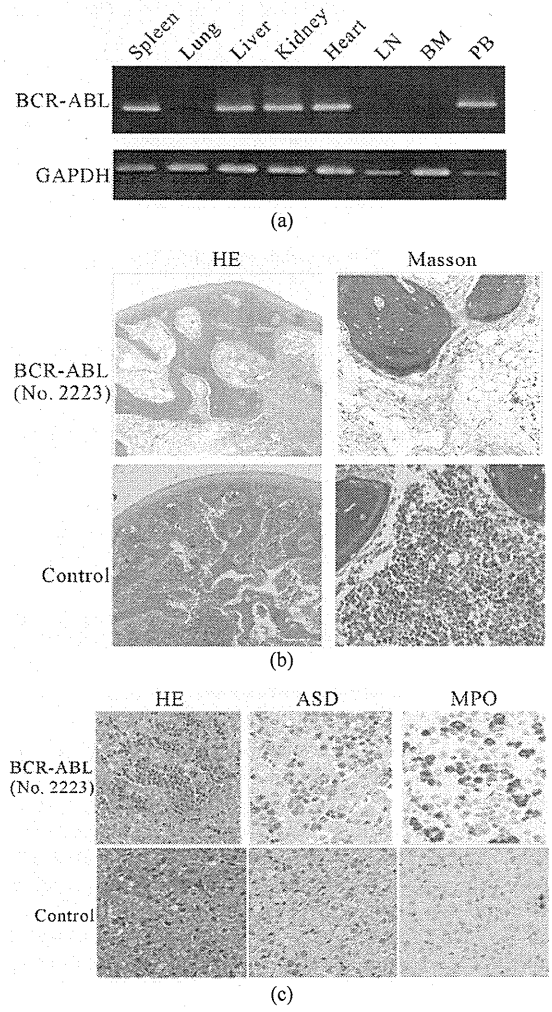

Figure 3. Pathological examination of marmoset No. 2223 (transduced using the *in vivo* BCR-ABL direct transduction method) with myelofibrosis-like disease. (a) Upper: Peripheral blood count of No. 2223 on day −7 before sacrifice. Data on the blood cell count of healthy marmosets were obtained from a textbook. Lower: The marmoset was sacrificed and pathologically examined on day 686 after p190 BCR-ABL was directly injected into the bone marrow. BCR-ABL gene expression was detected by a RT-PCR method in several organs. No. 2223: PGK-p190 BCR-ABL; (b) Left: Hematoxylin-Eosin (HE) staining of the bone marrow. Right: Masson staining. Bone marrow fibrosis is stained in blue. Upper: Experimental marmoset (No. 2223). Lower: Control marmoset; (c) Extramedullary hematopoiesis in the liver in the experimental marmoset (upper). ASD: Naphthol AS-D chloroacetate stain, MPO: Myeloperoxidase stain.

